

See discussions, stats, and author profiles for this publication at: <https://www.researchgate.net/publication/317081354>

# Statistical Distributions for the Corrosion Rates of Conventional and Prestressing Steel Reinforcement Embedded in Chloride Contaminated Mortar

**Article** in Corrosion -Houston Tx- · May 2017

DOI: 10.5006/2330

CITATIONS

0

READS

95

## 2 authors:



Jayachandran K

Aditya Birla Group

14 PUBLICATIONS 10 CITATIONS

[SEE PROFILE](#)



Radhakrishna Pillai

Indian Institute of Technology Madras

72 PUBLICATIONS 213 CITATIONS

[SEE PROFILE](#)

## Some of the authors of this publication are also working on these related projects:



Chloride Threshold of Prestressing Steel in Cementitious Systems with Ordinary Portland Cement, Fly Ash, and Corrosion Inhibitors [View project](#)



Electrochemical testing of steel-cementitious system [View project](#)

# Statistical Distributions for the Corrosion Rates of Conventional and Prestressing Steel Reinforcement Embedded in Chloride Contaminated Mortar

J. Karuppanasamy\* and R.G. Pillai†\*

## ABSTRACT

Many concrete structures are built using plain mild (PM) and cold-twisted deformed (CTD) steel rebars. Also, quenched and self-tempered (QST) and prestressing (PS) steels are extensively used in today's construction. For estimating the corrosion propagation period ( $t_p$ ) of concrete structures, the current practice is to assume that the corrosion rate ( $i_{\text{corr}}$ ) of different steels are equal to that of PM steel—leading to erroneous estimation of  $t_p$ . This paper provides  $i_{\text{corr}}$  data from a 33-month experiment on PM, CTD, QST, and PS steels embedded in chloride contaminated mortar. Linear polarization resistance test was adopted for  $i_{\text{corr}}$  measurement. A total of 100 specimens were tested. It was found that the CTD and QST steels exhibit higher  $i_{\text{corr}}$  than the PM and PS steels. The paper also provides statistical distributions for  $i_{\text{corr}}$  of these four steels. For PM, CTD, QST, and PS steel embedded in chloride contaminated mortar, and exposed to wet-dry conditions, these are found to be  $\sim$ Weibull (2.5, 20.7, 0)  $\mu\text{A}/\text{cm}^2$ ,  $\sim$ Lognormal (0.45, 3.2, 0)  $\mu\text{A}/\text{cm}^2$ ,  $\sim$ Gamma (6.8, 3.5, 0)  $\mu\text{A}/\text{cm}^2$ , and  $\sim$ Weibull 3P (1.3, 6.5, -0.02)  $\mu\text{A}/\text{cm}^2$ , respectively. Similar distributions for dry condition are also presented. These statistical tools would help engineers in estimating residual service life and scheduling repair activities.

**KEY WORDS:** cold-twisted deformed, concrete, corrosion propagation, corrosion rate, quenched and self-tempered (QST), plain mild steel, prestressing steels, statistical distribution, thermomechanically treated

## INTRODUCTION

The service life of structures can be defined as the duration for which the structure is able to meet the desired performance and safety. Most of the infrastructure projects are designed and built by considering a particular service life (or design life). However, many of the reinforced concrete structures are showing the signs of premature distress because of overloading, aging of materials, aggressive environmental conditions, inadequate maintenance, etc. The presence of oxygen, moisture, and chlorides at the surface of embedded steel reinforcing bars (i.e., rebar) can lead to the initiation of corrosion. Because of prolonged corrosion, the cover concrete can crack and spall. This can lead to further deterioration and reduction in the structural load carrying capacity. This increase in deterioration is indicated by the increase in the slope of the curve in Figure 1. The corrosion propagation period ( $t_p$ ) can be defined as the time required to initiate crack in the cover concrete and depends on the corrosion rate ( $i_{\text{corr}}$ ) of the embedded steel. Sometimes, the time available to repair the corroding structural elements is very short, once the corrosion is initiated. In order to avoid the unexpected/sudden failure and facilitate precautionary measures, the estimation of  $t_p$  and frequent monitoring of  $i_{\text{corr}}$  for these structures are essential.

This paper focuses on determining the probabilistic  $i_{\text{corr}}$  and  $t_p$  for the systems with the following four types of steel reinforcement that are widely used in the concrete structures. These are: (1) plain mild (PM), (2) cold-twisted deformed (CTD), (3) quenched and self-tempered (QST), and (4) prestressing (PS) steel

Submitted for publication: November 9, 2016. Revised and accepted: May 18, 2017. Preprint available online: May 18, 2017. <http://dx.doi.org/10.5006/2330>.

\* Corresponding author. E-mail: pillai@iitm.ac.in.

† Department of Civil Engineering, Indian Institute of Technology Madras, Chennai, India.

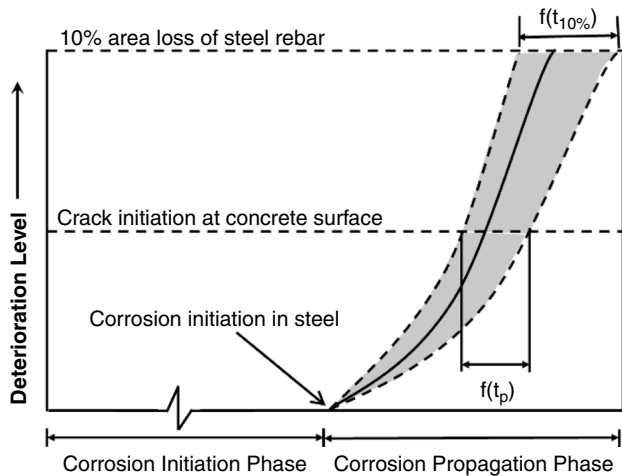


FIGURE 1. Representation of probabilistic corrosion propagation period.

reinforcement. The QST reinforcement is also known as thermomechanically treated (TMT) reinforcement, especially in the Indian subcontinent.

This paper is organized as follows. A review of the approaches for estimating the corrosion propagation period ( $t_p$ ) is provided next. Then, reviews of  $i_{\text{corr}}$  of various steel reinforcement and corrosion propagation models available in the literature are provided. Following this, the significance of this research and the details on the experimental program adopted to determine the  $i_{\text{corr}}$  are provided. Then, the experimental results and statistical distributions of  $i_{\text{corr}}$  of steels embedded in mortar and exposed to cyclic wet-dry and dry environments are provided. The probabilistic estimations on  $t_p$  (i.e., until crack initiation) and the time required for 10% and 15% reduction in tensile strength of PM, CTD, QST, and PS steel reinforcement are provided.

### Corrosion Propagation Models

Life 365<sup>†</sup> is a commonly used software program to estimate the service life and life-cycle cost of concrete structures exposed to chloride environments.<sup>1</sup> This software program assumes that  $t_p$  is equal to 6 y for all structures irrespective of steel and concrete used. This may not be conservative in many cases. Also, considering the random nature of corrosion process, a probabilistic approach for estimating  $t_p$  for different types of steel/cementitious system is required. Many corrosion propagation models are available in the literature.

Each estimation model may vary in their choice of input parameters and their approach of estimation. For example, the cracking behavior of concrete caused by the corrosion of steel was used in the nonlinear fracture models and/or finite element analysis.<sup>2-5</sup> However,

<sup>†</sup> Trade name.

such complicated mathematical models may not be preferred by the practicing engineers as they require many input parameters and additional skills to estimate  $t_p$ . A few other researchers have attempted to develop simple mathematical models and empirical formula to predict  $t_p$ . Parameters required for the  $t_p$  models developed by various researchers for different models are listed in Table 1.<sup>6-10</sup> Each model requires different input parameters as per the assumed corrosion mechanism and cracking process in concrete cover. In this paper, the Wang and Zhao<sup>5</sup> model that uses some of the most commonly and easily available parameters was considered for the estimation of  $t_p$ .

Wang and Zhao<sup>5</sup> have developed an empirical model with an assumption of constant corrosion rate to estimate  $t_p$ . This model assumes that the  $t_p$  ends when the first corrosion-induced crack occurs, as defined earlier in this paper. It is assumed that first crack occurs in concrete when the corrosion product reaches a certain quantity. Equation (1) gives the empirical formula suggested by Wang and Zhao<sup>5</sup> to estimate  $t_p$ .

$$t_p = \frac{H}{P_r} \quad (1)$$

$$H = \frac{\Delta}{\gamma} = \left[ \frac{\Delta}{0.33 \left( \frac{D}{C_v} \right)^{0.565} f_{cu}^{1.436}} \right] \quad (2)$$

$$P_r = \left( \frac{W}{F \rho_{st}} \right) i_{\text{corr}} \quad (3)$$

where  $t_p$  is time between corrosion initiation and the first cracking of cover concrete ( $\gamma$ ),  $H$  is the critical depth of rebar penetration (mm),  $\Delta$  is the critical thickness of corrosion product (mm),  $i_{\text{corr}}$  is the average corrosion rate ( $\text{A}/\text{mm}^2$ ),  $\gamma$  is the corrosion product expansion coefficient,  $D$  is initial diameter of the rebar (mm),  $C_v$  is the thickness of concrete cover (mm),  $f_{cu}$  is the cube strength of concrete ( $\text{N}/\text{mm}^2$ ),  $P_r$  is the penetration rate (mm/s),  $W$  is the equivalent weight of steel (g),  $F$  is the Faraday's constant (C), and  $\rho_{st}$  is the density of steel ( $\text{g}/\text{mm}^3$ ). Wang and Zhao<sup>5</sup> model assumed that the corrosion products will fill the steel/cementitious interface and develop an expansive pressure or tensile stress on the cover concrete, which will crack when the exerted tensile stress from the expansive corrosion product exceeds the tensile strength of the concrete.<sup>5</sup> This is empirically related to the compressive strength. The  $t_p$  can be predicted using this model using the  $i_{\text{corr}}$  data measured from the field and laboratory.

Andrade, et al.,<sup>6</sup> derived an empirical formula (Equation [4]) which uses the  $i_{\text{corr}}$  to calculate the

**TABLE 1**  
Input Parameters Required for Different Propagation Models

Sl. No	Parameters Considered	Wang and Zhao <sup>5</sup>	Bazant <sup>6</sup>	Morinaga <sup>7</sup>	Liu and Weyers <sup>8</sup>	Stratfull <sup>9</sup>	Clear <sup>10</sup>
1	Initial diameter of steel rebar	✓	✓	✓	✓		
2	Corrosion rate of steel rebar	✓	✓	✓	✓		
3	Density of steel rebar	✓	✓		✓		
4	Equivalent weight of steel rebar	✓	✓	✓			
5	Faraday's constant	✓	✓	✓			
6	Perimeter of steel rebar		✓	✓			
7	Bar hole flexibility		✓				
8	Poisson ratio of concrete		✓				
9	Elastic modulus of concrete		✓				
10	Concrete creep coefficient		✓				
11	Thickness of cover concrete			✓		✓	✓
12	Crack expansion coefficient of concrete	✓					
13	Cube strength of concrete	✓					
14	Depth of rebar penetration	✓					
15	Density of corrosion product				✓		
16	Thickness of corrosion products to generate the tensile stress on concrete				✓		
17	Mass of steel rebar corroded				✓		
18	Thickness of pore band around steel/concrete interface				✓		
19	Chloride concentration at surface					✓	✓
20	Water-cement ratio					✓	✓
21	Time of exposure						✓

reduction in the diameter of steel rebar after long-term exposure.

$$\phi_t = \phi_0 - 0.023 \times i_{\text{corr}} \times t \quad (4)$$

$\phi_t$  is the diameter of the rebar at time "t" after corrosion initiation and  $\phi_0$  is the initial diameter of reinforcement. Note that Equation (4) considers constant  $i_{\text{corr}}$ . However, this  $i_{\text{corr}}$  can vary with time, depending on the relative humidity (RH) and temperature variations prevailing in the different exposure conditions and inside concrete. Therefore, the prediction of  $t_p$  must consider the duration of wet and dry seasons prevailing at site in order to get realistic estimates.

#### Average Annual Corrosion Rate in the Field

In the current test program,  $i_{\text{corr}}$  data were measured at the end of each wet cycle followed by a dry period measurement. The  $i_{\text{corr}}$  at field conditions can vary as a function of the length of the annual rainy/sunny seasons (i.e., wet and dry periods). By considering the seasonal effects,  $i_{\text{corr,wet}}$  and  $i_{\text{corr,dry}}$ , the weighted average of annual corrosion rate ( $i_{\text{corr,annual}}$ ) is calculated as given in Equation (5):<sup>13</sup>

$$i_{\text{corr,annual}} = \alpha \times i_{\text{corr,wet}} + (1 - \alpha) \times i_{\text{corr,dry}} \quad (5)$$

where  $i_{\text{corr,wet}}$  = corrosion rate in wet conditions,  $i_{\text{corr,dry}}$  = corrosion rate in dry conditions, and  $\alpha$  = ratio of the duration of rainy-to-sunny season per year. The  $t_p$  estimated based on the  $i_{\text{corr,annual}}$  may better

represent the corrosion propagation mechanism that occurs in field conditions.

#### Corrosion Rates of Steel Reinforcement

Many researchers have been following the gravimetric mass loss method to obtain the average corrosion rate over the period of exposure (say, in mm/y). Nowadays, with the advancement of technology, the linear polarization resistance (LPR) tests can be conducted to represent the instantaneous corrosion rate or corrosion current density (say, in  $\mu\text{A}/\text{cm}^2$ ). Table 2 shows the  $i_{\text{corr}}$  for different steel reinforcement reported in literature.<sup>13-21</sup> These reported values exhibit significant scatter. The possible reasons for such huge

**TABLE 2**  
Corrosion Rates of Different Steel Reinforcement Reported in Literature<sup>(A)</sup>

Steel Type	Corrosion Rate	Reference
BS	2.54 $\mu\text{m}/\text{y}$	Spellman and Stratfull <sup>13</sup>
BS	94 $\mu\text{m}/\text{y}$	Clear <sup>14</sup>
BS	16 to 32 $\mu\text{m}/\text{y}$	Hladky, et al. <sup>15</sup>
BS	0.025 to 1.620 $\mu\text{m}/\text{y}$	Ismail and Ohtsu <sup>16</sup>
BS	1 to 2 $\mu\text{m}/\text{y}$	Hansson and Sorensen <sup>17</sup>
BS	0.026 to 1.575 $\mu\text{A}/\text{cm}^2$	Berke, et al. <sup>18</sup>
CTD	3 to 4.2 $\mu\text{A}/\text{cm}^2$	Pradhan and Bhattacharjee <sup>19</sup>
CTD	0.7 to 2.6 $\mu\text{A}/\text{cm}^2$	Firodiya, et al. <sup>20</sup>
MS	0.5 to 1.7 $\mu\text{A}/\text{cm}^2$	Firodiya, et al. <sup>20</sup>
PS	3 to 9 $\mu\text{A}/\text{cm}^2$	Karuppanasamy and Pillai <sup>21</sup>

<sup>(A)</sup> BS: black steel. CTD: cold-twisted deformed. MS: mild steel. PS: prestressing steel.

scatter are the differences in (i) chemical composition of steel, (ii) specimen design, (iii) test methods, (iv) experimental setup, (v) exposure conditions, etc., across the studies. For example, Soylev and Richardson<sup>22</sup> exposed the black steel rebar to 2%, 3%, and 4% of sodium chloride solution and found the  $i_{\text{corr}}$  as  $5.7 \mu\text{A}/\text{cm}^2$ ,  $6 \mu\text{A}/\text{cm}^2$ , and  $10.7 \mu\text{A}/\text{cm}^2$ , respectively. Pradhan and Bhattacharjee<sup>19</sup> reported that the  $i_{\text{corr}}$  of CTD reinforcement embedded in ordinary Portland cement (OPC) concrete with various water-cement ratios and different dosages of pre-mixed chlorides ranged from  $3 \mu\text{A}/\text{cm}^2$  to  $4 \mu\text{A}/\text{cm}^2$ . Pradhan and Bhattacharjee<sup>14</sup> also reported  $i_{\text{corr}}$  for the QST steel reinforcement embedded in concrete is within the range of  $2.5 \mu\text{A}/\text{cm}^2$  to  $6 \mu\text{A}/\text{cm}^2$ . Thus, the literature confirms that the  $i_{\text{corr}}$  may vary for different steel types, cementitious system, exposure conditions, and testing methods. Also, the statistical distribution of  $i_{\text{corr}}$  of various steels are necessary for realistic estimation of  $t_p$ .

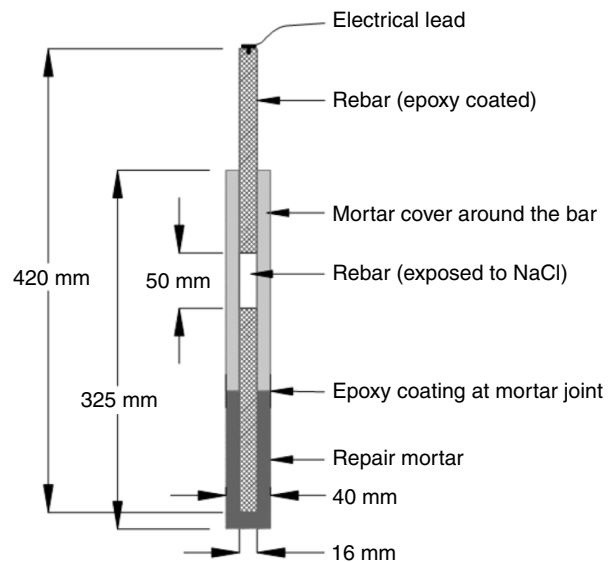
## RESEARCH SIGNIFICANCE

Service life of a structure can be defined as a sum of corrosion initiation period ( $t_i$ ) and corrosion propagation period ( $t_p$ ). Most of the reinforced concrete structures are built or being built using either PM, CTD, QST, or PS steel as reinforcement. The statistical distribution of  $i_{\text{corr}}$  is necessary for probabilistic estimation of  $t_p$ . However, very limited information is available on the  $i_{\text{corr}}$  of PM, CTD, QST, and PS steel reinforcement, making it difficult to estimate the  $t_p$ . Current practice is to assume similar  $i_{\text{corr}}$  for PM, CTD, QST, and PS steel, which may give erroneous estimations of probabilistic  $t_p$ . In addition, many software programs inadequately assume deterministic values for  $t_p$ , irrespective of the type of materials used in the structure. This paper provides experimental data and statistical distributions for  $i_{\text{corr}}$  of PM, CTD, QST, and PS steel reinforcement embedded in chloride contaminated mortar. These statistical distributions and probability density function (PDF) developed can be very valuable to budget and plan the maintenance, monitoring, and repair activities for the structures experiencing corrosion.

## EXPERIMENTAL PROGRAM

### Overview

A comprehensive corrosion test program was conducted to determine the probabilistic corrosion rate ( $i_{\text{corr}}$ ) of four types of steel reinforcement. Schematic of the test specimen is shown in Figure 2. Twenty-five specimens of each steel type, adding to a total of 100 specimens, were cast. The cast specimens were cured for 28 d and then subjected to cyclic wet-dry exposure using 3.5% sodium chloride solution for a period of



Note: For prestressing steel specimens, the diameter of the steel piece and mortar cylinder were 5.2 mm and 29.2 mm, respectively.

**FIGURE 2.** Corrosion test specimen with a steel bar embedded in mortar.

24 months. Every month, at the end of wet period, the corrosion rate ( $i_{\text{corr,wet}}$ ) of each specimen was measured using linear polarization technique. Also, the specimens were then allowed to dry in the standard laboratory environment until the end of the 33rd month. The corrosion rate ( $i_{\text{corr,dry}}$ ) was measured at the 27th and 33rd month. These data were used to develop a statistical distribution of  $i_{\text{corr,wet}}$  and  $i_{\text{corr,dry}}$ , which were later used to estimate probabilistic  $t_p$ . The details of the materials used, casting, exposure conditions, test procedure, etc., are described next.

### Materials Used

The mortar with water:cement:sand ratio of 0.55:1:2.75 and an average compressive strength of about 30 MPa was used. The initial and final setting time of the 53 Grade OPC cement was 52 min and 265 min, respectively. The fineness value was  $310 \text{ m}^2/\text{kg}$ , as per ASTM C204.<sup>23</sup> The oxide composition of the OPC cement was determined by x-ray fluorescence spectroscopy (see Table 3). Standard silica sand (known as Ennore sand in India) of Grades I, II, and III, as classified in IS:383<sup>24</sup> was used. Distilled water was used for preparing the mortar and chloride solutions. Table 4 shows the chemical composition (determined using optical emission spectroscopy) of PM, CTD, QST, and PS steel reinforcement used for this study.

### Specimen Design and Preparation

The schematic of the specimen is shown in Figure 2. The PM, CTD, and QST reinforcement (with

**TABLE 3**

Chemical Composition of 53 Grade Ordinary Portland Cement (OPC) Used

Ingredients	Concentration (%)
CaO	66.67
SiO <sub>2</sub>	18.91
Fe <sub>2</sub> O <sub>3</sub>	4.94
Al <sub>2</sub> O <sub>3</sub>	4.51
SO <sub>3</sub>	2.5
MgO	0.87
K <sub>2</sub> O	0.43
Na <sub>2</sub> O	0.12
Loss of ignition	1.05

**TABLE 4**

Chemical Composition of PM, CTD, QST, and PS Steel Reinforcement Used<sup>(A)</sup>

Element	PM	CTD	QST	PS
Cu	0.27	0.09	0.16	0.02
Co	–	0.01	0.02	0.01
Al	–	0.01	0.03	0.04
Ni	0.09	0.07	0.15	0.02
Mo	0.02	0.01	0.06	0.00
Cr	0.08	0.07	0.24	0.27
S	0.05	0.27	0.01	0.00
P	0.06	0.09	0.08	0.06
Mn	0.64	0.45	0.63	0.83
Si	0.26	0.23	0.24	0.29
C	0.19	0.13	0.2	0.84
Fe	Re.	Re.	Re.	Re.

<sup>(A)</sup> Re.: Remaining.

16 mm diameter and 420 mm long) and king wire (5.2 mm diameter and 420 mm long) removed from a 7-wire PS strand were used to prepare the test specimens. The steel reinforcement was cleaned by immersing in ethanol and using an ultrasonic cleaner for 5 min—to maintain “as-received condition.” To facilitate corrosion measurements, an insulated copper wire (300 mm long) was fastened to one end of the steel specimen using a metallic screw. Then, the steel bar (except the 50 mm length at the center) and the screw were coated with two thin layers of a low viscosity epoxy (Sikadur<sup>®</sup>-52 UF<sup>†</sup>). The steel reinforcement was then embedded in mortar.

### Curing and Exposure Conditions

The test specimens were cured in a laboratory environment (ambient temperature = 25±3°C and RH = 65±5%) for 24±1 h after casting. After this, the specimens were immersed/cured by immersing in saturated limewater for additional 27 d. Then, the cured specimens were subjected to cyclic wet-dry exposure (i.e., 7 d wetting followed by 7 d drying) using 3.5% sodium chloride solution and in a laboratory environment with ~65% RH and ~25°C. During the wet period, the specimens were kept in a plastic container

with sodium chloride solution. This container was covered with a plastic lid to avoid evaporation. During the dry period, the specimens were placed outside of this container. The wet-dry exposure was continued for a period of 24 months under the laboratory environment. Later, the specimens were allowed to completely dry and the corrosion rates were measured at the 27th month and 33rd month.

Unfortunately, after 10 months of exposure, the 2-layer epoxy coating at the bottom end portion of the steel specimens (a lower region with no mortar cover; see Figure 2) failed/cracked and led to severe underfilm or crevice corrosion (i.e., beneath the epoxy layer). This was a result of the poor long-term performance of epoxy coating; the specimens exhibited large scatter in the  $i_{\text{corr}}$  data. The  $i_{\text{corr}}$  data obtained during this period do not truly represent the actual corrosion rate at the predefined exposed surface (center 50 mm long) of the specimen. Therefore, the damaged epoxy coating and the underfilm or crevice corrosion products were removed by following the procedure given in ASTM G1-16 (Designation C.3.5 in Table A1.1)<sup>25</sup> and re-coated with two new layers of epoxy. To avoid further failure/cracking of the epoxy coating, the bottom part of the epoxy coated steel was covered with cement mortar (denoted as “repair mortar” in Figure 2). The interface between the old and new mortar was also sealed with epoxy. After 28 d of curing of the repair mortar, the repaired specimens were again exposed to cyclic wet-dry conditions using 3.5% sodium chloride solution and corrosion rate measurement was resumed after the 18th month. During the period from the 10th month to the 18th month of exposure, the specimens were stored in the laboratory environment (~65% RH and ~25°C). However, it should be noted that only the  $i_{\text{corr}}$  measured from the 19th month to the 24th month was used for the development of statistical distribution in this paper.

### Corrosion Test Setup and Corrosion Rate Measurements

Figure 3 shows the three-electrode corrosion cell with a working electrode (WE), a counter electrode (CE), and a reference electrode (RE). All of the electrodes were placed in a glass beaker with 3.5% sodium chloride solution. Then the corrosion cell setup was connected to a potentiostat and computer. The central 50 mm long uncoated region of the steel piece was considered as the WE. A 90 mm diameter and 50 mm long pipe (annular setup) made of Nichrome wire mesh (24 wires of 0.5 mm diameter per in) was used as the CE. The test specimen was placed at the center of the annular CE. The saturated calomel electrode (SCE) was used as the RE and placed near the surface of mortar cylinder (near the uncoated steel portion at the center 50 mm).

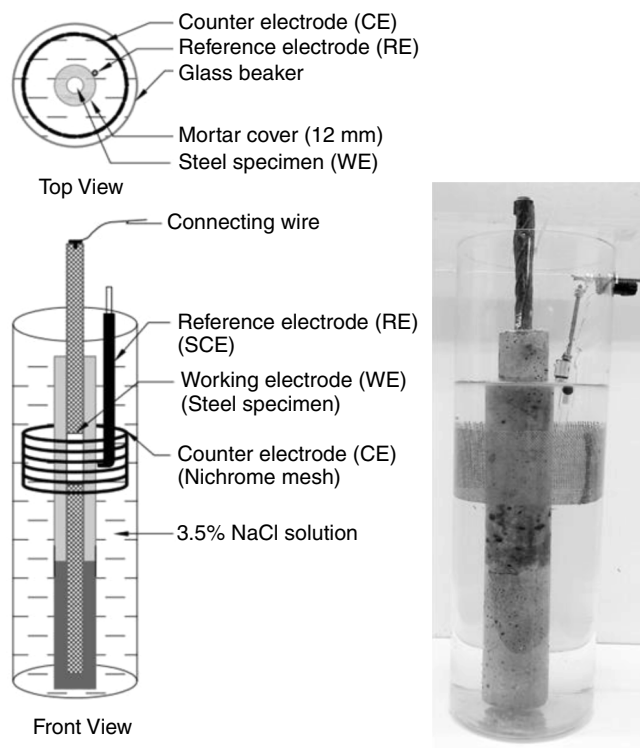


FIGURE 3. Schematic of the three-electrode corrosion cell setup.

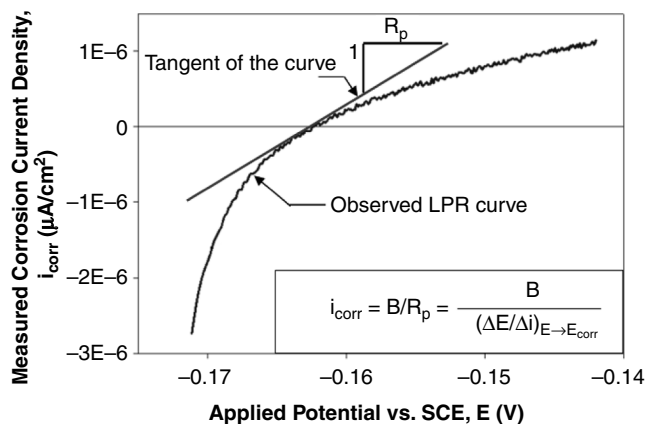


FIGURE 4. A typical LPR curve.

Corrosion measurements were made at the end of the alternate wetting period (say, once in a month). At first, the open-circuit potential (OCP) of the steel specimen was measured. Immediately after measuring the OCP, the LPR test was conducted with a scan range of 15 mV to  $-15$  mV with respect to the measured OCP and at a scan rate of  $0.1667$  mV/s. The measured corrosion current density ( $i$ ) was plotted with respect to the applied potential ( $E$ ) to generate the LPR curve (see Figure 4 for a typical LPR curve). The  $i_{\text{corr}}$  was calculated as follows.

$$i_{\text{corr}} = \frac{B}{R_p} = \frac{B}{(\Delta E/\Delta i)_{E \rightarrow E_{\text{corr}}}} \quad (6)$$

where  $B$  is the Stern-Geary coefficient,  $R_p$  is the polarization resistance,  $E$  is the applied potential, and  $i$  is the measured corrosion current density.  $B$  is assumed as  $26$  mV for all of the measurements.

**Corrosion Rate Measured During the Wet-Dry Cycle and the Dry Period** — The specimens were exposed to 7 d wet and 7 d dry cycle. The  $i_{\text{corr}}$  values measured at the end of every 2nd wet cycle from the 19th month to the 24th month are used as the corrosion rate during wet period (denoted as  $i_{\text{corr,wet}}$ ). From the 25th month to the 33rd month, the specimens were allowed to dry in a laboratory environment (temperature =  $25 \pm 3^\circ\text{C}$  and RH =  $65 \pm 5\%$ ) and the  $i_{\text{corr}}$  were measured at the 27th month and the 33rd month. These were considered as the corrosion rate for dry period (denoted as  $i_{\text{corr,dry}}$ ). Note that the dry specimens were wetted by placing in a glass beaker with 3.5% sodium chloride solution for 30 min prior to the electrochemical testing. Only the  $i_{\text{corr,wet}}$ , and  $i_{\text{corr,dry}}$  data were used for estimating  $t_p$ , provided later in this paper.

## RESULTS AND DISCUSSION

### Measured Corrosion Rate of Different Steels in Laboratory

As mentioned earlier, this paper focuses only on  $t_p$ , which mainly depends on the  $i_{\text{corr}}$  of embedded steel reinforcement embedded in mortar. Figure 5 shows the average OCP of PM, CTD, QST, and PS steel reinforcement measured until the 33rd month. After 2 months of exposure, corrosion potential ( $E_{\text{corr}}$ ) values were more negative than  $-276$  mV<sub>SCE</sub> (equivalent to  $-350$  mV<sub>Cu/CuSO4</sub> electrode) and exhibited a significant reduction in OCP when compared to initial readings. This indicates that the specimens are possibly experiencing “active” corrosion. Also, all of the steels exhibited similar OCP values. Figure 6 shows the average  $i_{\text{corr}}$  of the different steels exposed to chloride environment. After 5 months of exposure, the  $i_{\text{corr}}$  of steel specimens started showing huge scatter in the measured  $i_{\text{corr}}$ . This phenomenon is a result of the failure of the epoxy coating provided at the bottom portion of the steel bar. Later, the specimens were repaired as described in the *Curing and Exposure Conditions* section. The corrosion testing was resumed from the 18th month onward until 33 months. At the end of 33 months of exposure, corrosion stains were visible on the surface of test specimens. However, they did not exhibit cracking—even with severe corrosion. The probable reasoning could be as follows. The overall/effective permeability of concrete could be less than that of mortar with similar paste quality, because of the presence of impermeable coarse

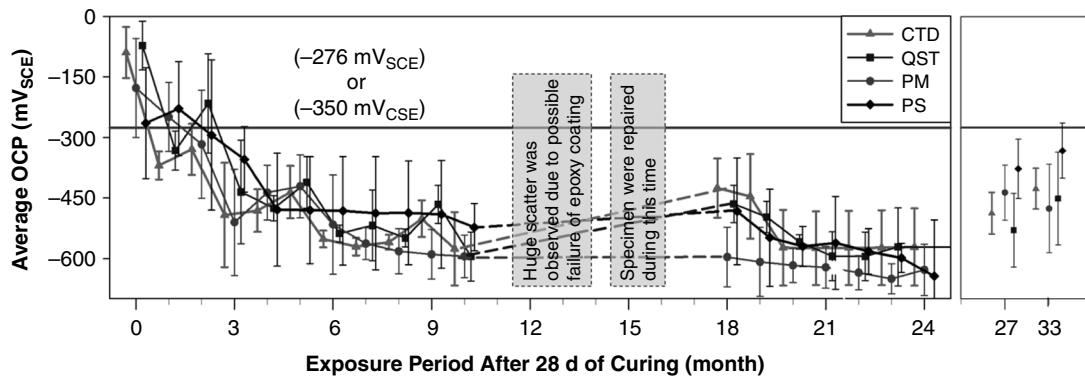


FIGURE 5. Average corrosion potential of PM, CTD, QST, and PS bars.

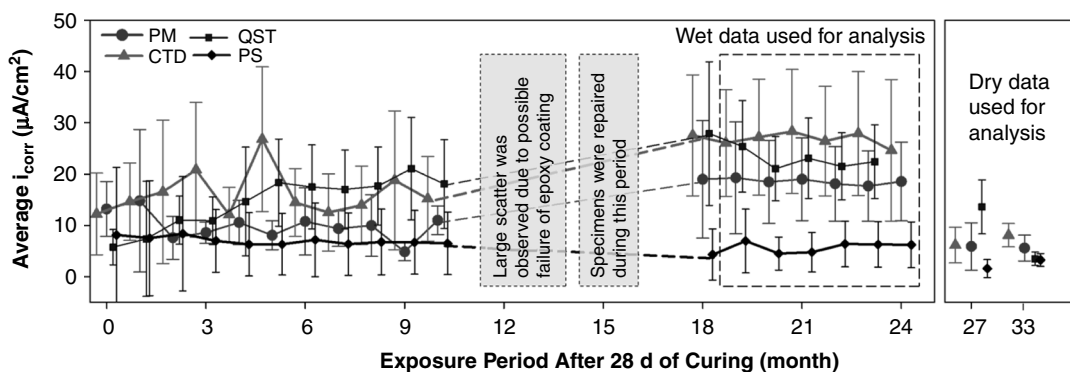


FIGURE 6. Average corrosion current density of PM, CTD, QST, and PS bars.

aggregates occupying about 70% of volume. In the case of test specimens, the corrosion products could easily permeate through the relatively more permeable 12 mm thick mortar cover without building up expansive pressure and cracking. Although the pressure buildup and eventual cracking mechanisms (in the bulk cover material) are different in the steel-mortar and steel-concrete systems, the corrosion rate (an interface property) from steel-mortar systems can be used for estimating the corrosion propagation time in steel-concrete systems.

#### $i_{\text{corr,wet}}$ Measurements

Figure 7(a) shows the dot plot of the measured  $i_{\text{corr,wet}}$  of PM, CTD, QST, and PS steel reinforcement measured at the end of each wet period during cyclic wet-dry exposure from the 19th month to the 24th month. The average  $i_{\text{corr,wet}}$  of PM steel reinforcement is about  $19 \mu\text{A}/\text{cm}^2$  with coefficient of variation (COV) of 0.44. The  $i_{\text{corr,wet}}$  data obtained for CTD steel reinforcement exhibited huge scatter with a mean of  $27 \mu\text{A}/\text{cm}^2$  and COV of 0.44. The  $i_{\text{corr,wet}}$  data obtained for QST steel reinforcement exhibited a mean value of  $24 \mu\text{A}/\text{cm}^2$  and COV of 0.38. Similarly, the PS steel reinforcement showed the average  $i_{\text{corr,wet}}$  of

$6 \mu\text{A}/\text{cm}^2$  and COV of 0.77. The results showed higher  $i_{\text{corr,wet}}$  values when compared to the value reported in literature. However, the average  $i_{\text{corr}}$  in the real structure would be different from the instantaneous corrosion rate measured in the severe laboratory conditions. This is taken into consideration during the estimation of  $t_p$  later in this paper (see *Parametric Studies and Probability Density Function of  $t_p$*  section)

#### $i_{\text{corr,dry}}$ Measurements

Figure 7(b) shows the dot plot of the measured  $i_{\text{corr,dry}}$  of PM, CTD, QST, and PS steel reinforcement. The average  $i_{\text{corr,dry}}$  of PM steel reinforcement is about  $5.3 \mu\text{A}/\text{cm}^2$  with a COV of 0.63. The  $i_{\text{corr,dry}}$  data obtained for CTD steel reinforcement exhibited huge scatter with a mean of  $7 \mu\text{A}/\text{cm}^2$  and COV of 0.43. The  $i_{\text{corr,dry}}$  data obtained for QST steel reinforcement exhibited a mean value of  $8.6 \mu\text{A}/\text{cm}^2$  and COV of 0.74. Similarly, the PS steel reinforcement showed the average  $i_{\text{corr,dry}}$  of  $2.5 \mu\text{A}/\text{cm}^2$  with COV of 0.7. In short, the  $i_{\text{corr,wet}}$  was  $\sim 2.5$  times higher than the average of  $i_{\text{corr,dry}}$  for QST and PS steel reinforcement. Similarly, the average  $i_{\text{corr,wet}}$  was  $\sim 3$  and 4 times higher than  $i_{\text{corr,dry}}$  for PM and CTD steel reinforcement, respectively.



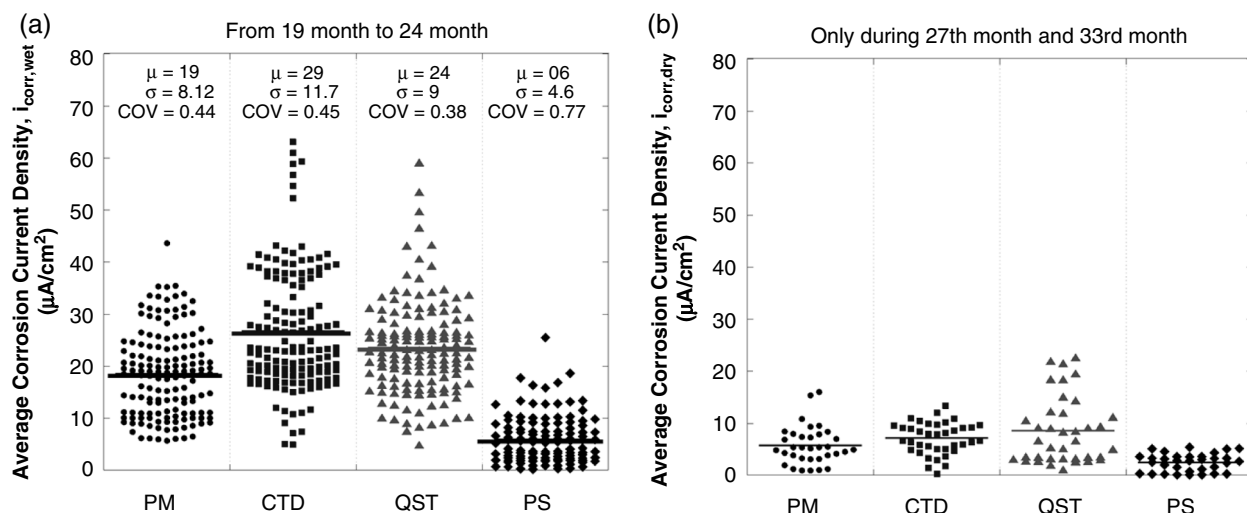


FIGURE 7. Corrosion rates of various steels.

The CTD steel reinforcement experienced higher average corrosion rates than QST steel reinforcement. This may be because the CTD steel reinforcement is strain-hardened or cold-twisted during the manufacturing process to increase the yield strength. This process can lead to residual stresses and surface defects (at the microstructure level), which can lead to corrosion when exposed to aggressive environments. The PM and PS steel reinforcement have smooth surfaces (i.e., without any ribs), and no residual stresses at the surface. Hence, they show less  $i_{\text{corr}}$  when compared to other steels. The difference in chemical composition may be another reason for the low corrosion rate.

#### Average Annual Corrosion Rate in the Field

By considering the seasonal effects,  $i_{\text{corr,wet}}$ , and  $i_{\text{corr,dry}}$ , the weighted average of annual corrosion rate ( $i_{\text{corr,annual}}$ ) is calculated as given in Equation (6). The  $t_p$  was estimated based on the  $i_{\text{corr,annual}}$ , which may better represent the corrosion propagation mechanism that occurs in field conditions. Thus, the  $i_{\text{corr,annual}}$  is used for the case study presented later in the

Parametric Studies and Probability Density Function of  $t_p$  section.

#### Statistical Distributions of Corrosion Rate of Different Steels

For simulation purpose,  $i_{\text{corr}}$  should be treated as a positive real number. Hence, choosing a normal distribution for the  $i_{\text{corr}}$  is mathematically incorrect. This is because the random data generated using a normal distribution might have negative numbers and can cause mathematical difficulties during simulation studies.<sup>26</sup> Also, Shapiro-Wilkinson normality tests on the  $i_{\text{corr,wet}}$  and  $i_{\text{corr,dry}}$  data sets for PM, CTD, QST, and PS steel reinforcement concluded that the data sets do not follow a normal distribution. To find appropriate statistical distributions, the software package Easy-Fit<sup>†,22</sup> was used. Based on the Kolmogorov-Smirnov (K-S) goodness of fit test (see Table 5), the data sets were ranked with different statistical distributions that are commonly used (e.g., Gaussian, Weibull, Gamma, Normal, and Lognormal) The measured  $i_{\text{corr,wet}}$  data for PM, CTD, QST, and PS steel reinforcement fit well with Weibull, Lognormal, Gamma, and Weibull 3P

TABLE 5  
Goodness of Fit for  $i_{\text{corr}}$  of PM, CTD, QST, and PS Steel Reinforcement<sup>(A)</sup>

	$i_{\text{corr,wet}}$				$i_{\text{corr,dry}}$			
	PM	CTD	QST	PS	PM	CTD	QST	PS
Normal	4	7	7	7	6	2	7	1
Lognormal	7	1	5	6	5	6	5	7
Lognormal 3P	2	3	2	5	1	3	3	2
Weibull	1	6	4	3	3	7	4	3
Weibull 3P	3	5	6	1	4	1	2	4
Gamma	5	2	1	2	2	5	6	5
Gamma 3P	6	4	3	4	7	4	1	6

<sup>(A)</sup> Wet data measurements from the 19th through 24th months. Dry data measurements from the 27th and 33rd month.

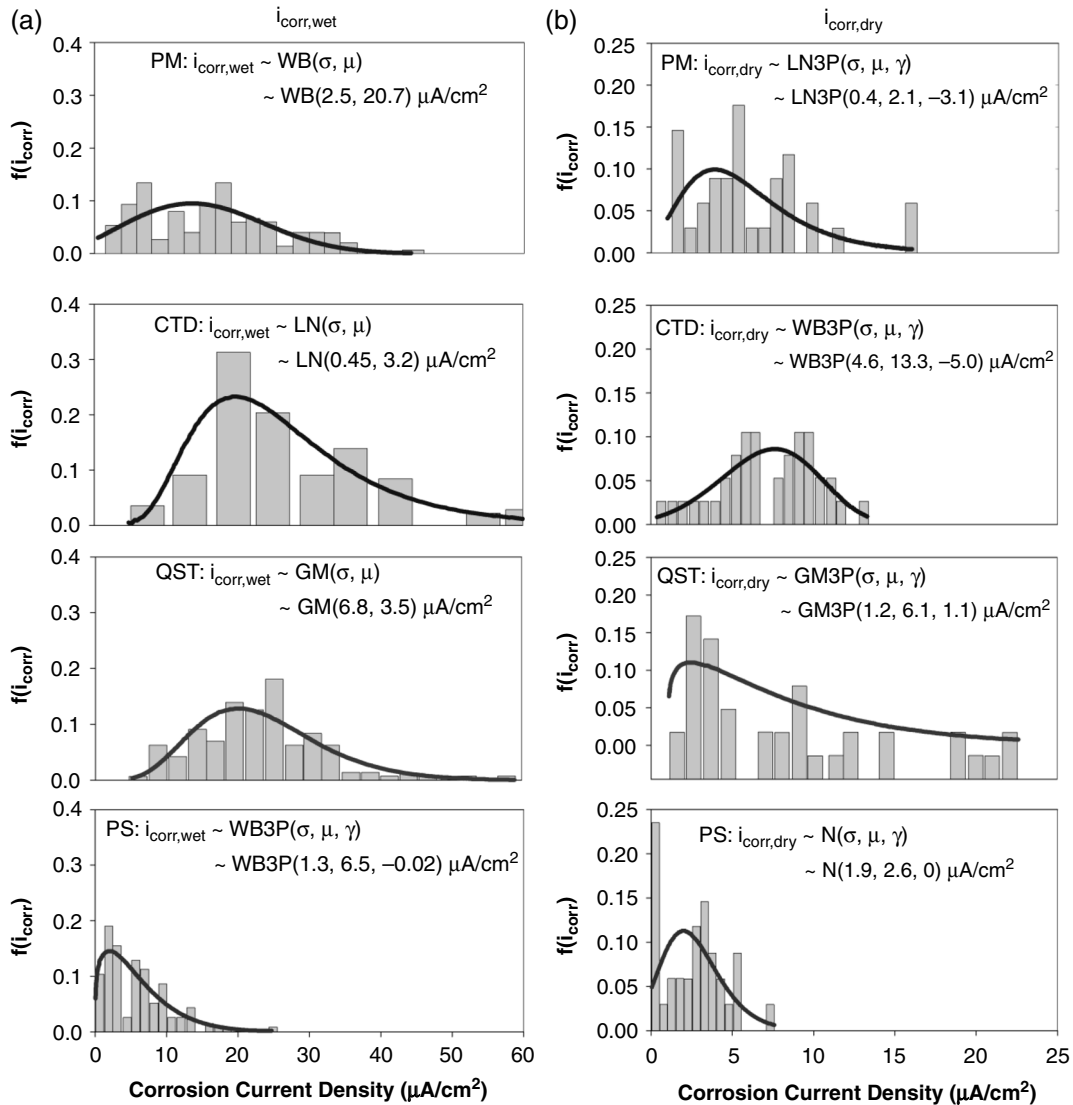


FIGURE 8. Distributions for  $i_{corr,wet}$  and  $i_{corr,dry}$  of various steel reinforcement.

TABLE 6

Summary of Distributions Based on the Corrosion Rate of Different Steel Reinforcement Exposed from 19 to 24 Months

Steel Type	Distribution (D)	Parameter $\sim D(\sigma, \mu, \gamma)$ in $\mu\text{A}/\text{cm}^2$
PM	Weibull	$\sim \text{WB}(2.5, 20.7, 0)$
CTD	Lognormal	$\sim \text{LN}(0.45, 3.2, 0)$
QST	Gamma	$\sim \text{GM}(6.8, 3.5, 0)$
PS	Weibull 3P	$\sim \text{WB3P}(1.3, 6.5, -0.02)$

distributions, respectively. Similarly,  $i_{corr,dry}$  data for PM, CTD, QST, and PS steel reinforcement fit well with Lognormal 3P, Weibull 3P, Gamma, and Normal distributions, respectively.

Figures 8(a) and (b) show the histograms and the PDFs for  $i_{corr,wet}$  and  $i_{corr,dry}$ , respectively, of PM, CTD,

TABLE 7

Summary of Distributions Based on the Corrosion Rate of Different Steel Reinforcement Measure at 27th and 33rd Month

Steel Type	Distribution (D)	Parameter $\sim D(\sigma, \mu, \gamma)$ in $\mu\text{A}/\text{cm}^2$
PM	Lognormal 3P	$\sim \text{LN3P}(0.4, 2.1, -3.1)$
CTD	Weibull 3P	$\sim \text{WB3P}(4.6, 13.3, -5)$
QST	Gamma 3P	$\sim \text{GM3P}(1.2, 6.1, 1.1)$
PS	Normal	$\sim \text{N}(1.9, 2.6, 0)$

QST, and PS steel reinforcement. Tables 6 and 7 show the statistical parameters for  $i_{corr,wet}$  and  $i_{corr,dry}$  arrived for each steel type. A significant difference is observed between the  $i_{corr,wet}$  and  $i_{corr,dry}$ . The variation in the type of distribution and the change in the statistical

TABLE 8

Parameters Considered for Estimating  $t_i$  Using Wang and Zhao<sup>5</sup>

Parameters	Unit	Value
Cover depth ( $C_v$ )	mm	50
Compressive strength of concrete ( $f_{cu}$ )	MPa	30
Initial steel diameter (D)	mm	16 for PM, CTD, QST; 5.2 for PS
Equivalent weight of steel (W)	g	27.92
Faraday's constant (F)	Coulombs	96,500
Density of steel ( $\rho_{st}$ )	gm/cm <sup>3</sup>	7.85
Crack expansion coefficient of concrete ( $\gamma$ )		3.02

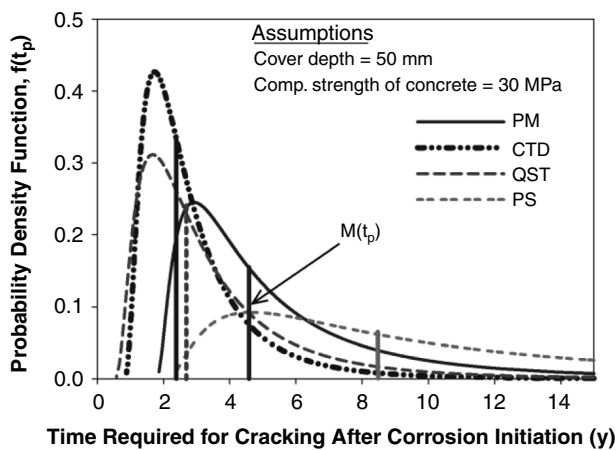


FIGURE 9. Estimated crack initiation period based on  $i_{corr,annual}$ .

parameters clearly shows that the use of same corrosion rate and considering a normal distribution for all of the steel types will lead to an erroneous estimation of  $t_p$ .

### Parametric Studies and Probability Density Function of $t_p$

**Probabilistic Estimation of  $t_p$  to Initiate Crack in Cover Concrete** — As mentioned earlier in Table 1, Wang and Zhao<sup>5</sup> considered the  $i_{corr}$ , cover depth ( $C_v$ ), and

compressive strength ( $f_{cu}$ ) as the major influencing parameters to estimate  $t_p$ .<sup>5</sup> In this analysis, the statistical distributions of  $i_{corr,annual}$  for different steel was used, which was calculated from  $i_{corr,wet}$  and  $i_{corr,dry}$  using Equation (4). The input parameters required for Wang and Zhao<sup>5</sup> model are listed in Table 8. The  $t_p$  for concrete systems with different steel reinforcement was estimated using the model by Wang and Zhao.<sup>5</sup> A typical south Indian climate, in which 1 y can be divided into 3 month of wet season and 9 month of dry season is considered for this parametric study.

Figure 9 shows the PDF of  $t_p$  obtained for the systems with PM, CTD, QST, and PS steel reinforcement. Note that these PDFs are skewed to the right. For skewed distributions, the median is a better statistic than the mean or average and the vertical lines within the PDF curves indicate the median values, which are herein denoted as  $M(t_p)$ . The model by Wang and Zhao<sup>5</sup> estimates that the  $M(t_p)$  for concrete structures with PM, CTD, QST, and PS steel reinforcement are 4.5, 2.4, 2.7, and 8.5 y, respectively.

### Probabilistic Estimation of $t_p$ for a Particular Reduction in Cross-Sectional Area ( $t_{p,\Delta\%}$ )

In reinforced concrete structures, when the loss in the cross-sectional area of steel reinforcement exceeds  $\approx 10\%$  of the nominal cross-sectional area, the structure may reach an unsafe level and major repair/replacement of steel is needed. That is, 10% loss in cross-sectional area is approximately equal to 10% reduction in tensile strength of steel rebars. When such a state is reached, repair/rehabilitation/retrofitting work is recommended because of the limited safety margins. Thus, the reduction in  $t_p$  with the corresponding percent reduction in the cross-sectional area ( $\Delta\%$ ) of the rebar is studied and represented as  $t_{p,\Delta\%}$ . The study was conducted for  $\Delta\%$  of 5, 10, and 15% and the PDF for the four steel were developed.

Once the crack is initiated, the rate of corrosion propagation may vary significantly, as the availability of moisture and oxygen is expected to be high. However, in this study, the  $t_{p,5\%}$ ,  $t_{p,10\%}$ , and  $t_{p,15\%}$  were estimated

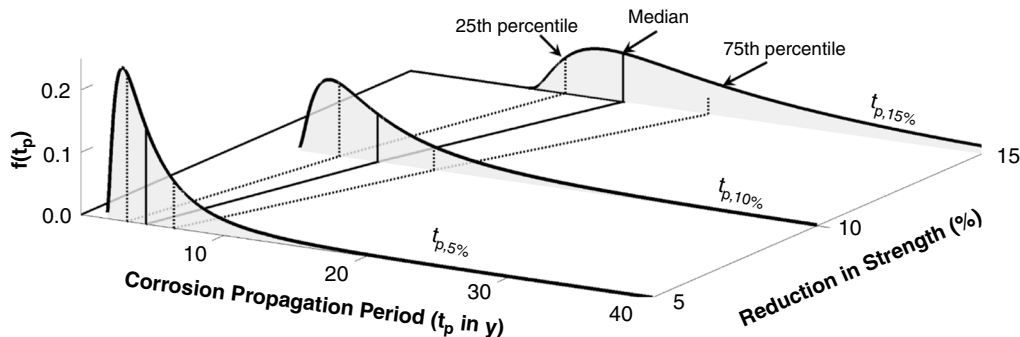


FIGURE 10.  $t_{p,5\%}$ ,  $t_{p,10\%}$ , and  $t_{p,15\%}$  loss in PM steel rebar with reference to exposure period.

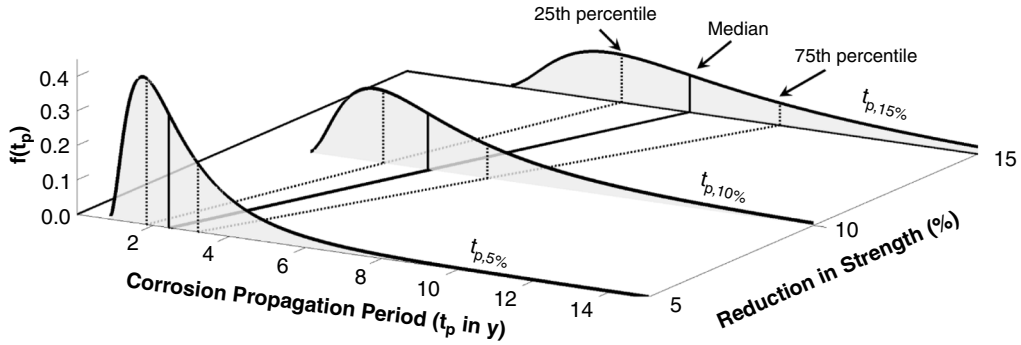


FIGURE 11.  $t_{p,5\%}$ ,  $t_{p,10\%}$ , and  $t_{p,15\%}$  loss in CTD steel rebar with reference to exposure period.

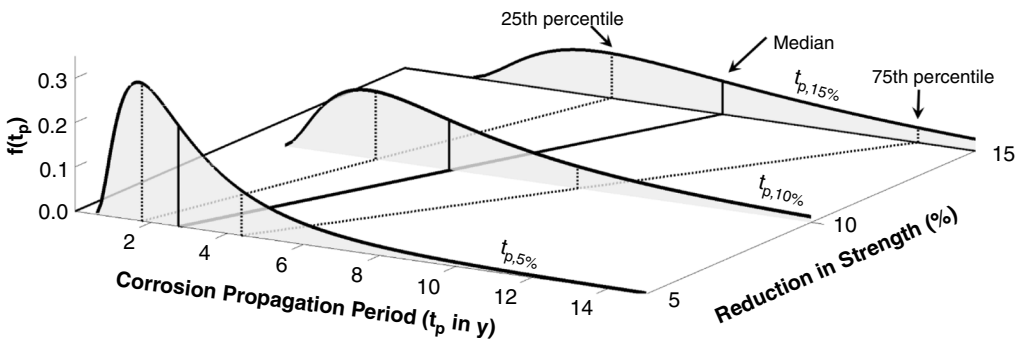


FIGURE 12.  $t_{p,5\%}$ ,  $t_{p,10\%}$ , and  $t_{p,15\%}$  loss in QST steel rebar with reference to exposure period.

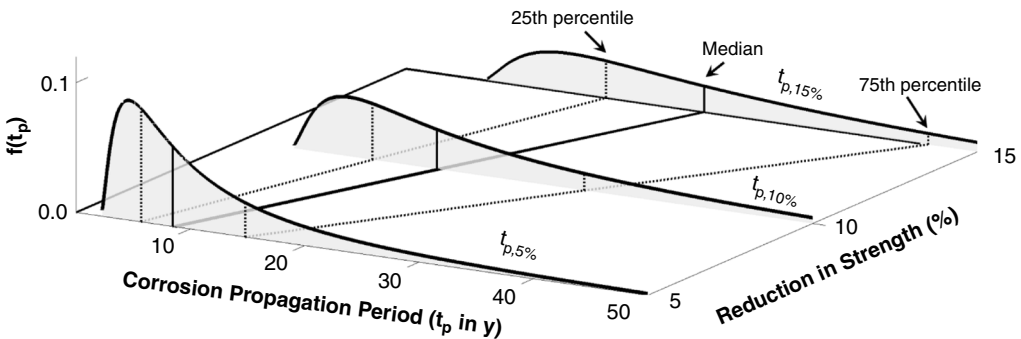


FIGURE 13.  $t_{p,5\%}$ ,  $t_{p,10\%}$ , and  $t_{p,15\%}$  loss in PS steel rebar with reference to exposure period.

using Equation (4)<sup>6</sup> by assuming a linear corrosion propagation mechanism and constant  $i_{\text{corr,annual}}$  determined from  $i_{\text{corr,wet}}$  and  $i_{\text{corr,dry}}$  using Equation (4). Figures 10 through 13 shows the probability of  $M(t_{p,5\%})$ ,  $M(t_{p,10\%})$ , and  $M(t_{p,15\%})$  for different steel reinforcement after the corrosion initiation. In the PDFs, the vertical solid line from the abscissa denotes the median (50th percentile), which is  $M(t_p)$  and the dotted vertical lines along the left and right side of the solid line denotes the 25th percentile and 75th percentile, respectively, of the estimated corrosion propagation period.

Figure 10 shows the probability of  $M(t_{p,5\%})$ ,  $M(t_{p,10\%})$ , and  $M(t_{p,15\%})$  for PM steel reinforcement after the corrosion initiation. Based on the probabilistic estimation, the  $M(t_{p,5\%})$ ,  $M(t_{p,10\%})$ , and  $M(t_{p,15\%})$  for a concrete system with PM steel is about 4.5, 9, and 15 y, respectively. Figure 11 shows the probability of  $M(t_{p,5\%})$ ,  $M(t_{p,10\%})$ , and  $M(t_{p,15\%})$  for CTD steel reinforcement after the corrosion initiation. The concrete system with CTD steel reinforcement may have  $M(t_{p,5\%})$ ,  $M(t_{p,10\%})$ , and  $M(t_{p,15\%})$  as 2.5, 5, and 7.5 y, respectively. The concrete system with QST steel may

have  $M(t_{p,5\%})$ ,  $M(t_{p,10\%})$ , and  $M(t_{p,15\%})$  of 3, 5.5, and 9 y, respectively, as shown in Figure 12. As shown in Figure 13, the  $M(t_{p,5\%})$ ,  $M(t_{p,10\%})$ , and  $M(t_{p,15\%})$  in the concrete system with PS steel reinforcement is around 8.5, 17, and 26 y, respectively.

Therefore, instead of assuming  $t_p$  as 6 y, it is recommended that the probabilistic distributions for  $i_{\text{corr,wet}}$  and  $i_{\text{corr,dry}}$  presented in this paper and a suitable model may be used to estimate  $t_p$  for structures with different steel reinforcement.

## CONCLUSIONS

Based on the experimental results and the corrosion propagation models discussed in this paper, the following conclusions are drawn.

❖ When embedded in similar cementitious system to that used in the present experiment and when subjected to a wet cycle exposure to chloride environment, the corrosion rate,  $i_{\text{corr,wet}}$ , of PM, CTD, QST, and PS steel reinforcement can be statistically expressed as follows:

- I. PM:  $\sim$ Weibull (2.5, 20.7, 0)  $\mu\text{A}/\text{cm}^2$ .
- II. CTD:  $\sim$ Lognormal (0.45, 3.2, 0)  $\mu\text{A}/\text{cm}^2$ .
- III. QST:  $\sim$ Gamma (6.8, 3.5, 0)  $\mu\text{A}/\text{cm}^2$ .
- IV. PS:  $\sim$ Weibull 3P (1.3, 6.5, -0.02)  $\mu\text{A}/\text{cm}^2$ .

❖ When embedded in similar cementitious system to that used in the present experiment and when subjected to a dry exposure, the corrosion rate,  $i_{\text{corr,dry}}$ , of PM, CTD, QST, and PS steel reinforcement can be statistically expressed as follows:

- I. PM:  $\sim$ Lognormal (0.4, 2.1, -3.1)  $\mu\text{A}/\text{cm}^2$ .
- II. CTD:  $\sim$ Weibull 3P (0.46, 13.3, -5)  $\mu\text{A}/\text{cm}^2$ .
- III. QST:  $\sim$ Gamma 3P (1.2, 6.1, 1.1)  $\mu\text{A}/\text{cm}^2$ .
- IV. PS:  $\sim$ Normal (1.9, 2.6, 0)  $\mu\text{A}/\text{cm}^2$ .

❖ Using the statistical distributions mentioned above and the Wang and Zhao<sup>5</sup> model, the median time required to crack the cover concrete  $M(t_p)$  is about 1.5 times higher in the case of PM and PS steel reinforcement than that in the case of CTD and QST steel reinforcement.

❖ The median time required for 10% reduction in tensile strength is around 1.2 times higher in PM and PS steel reinforcement when compared to CTD and QST steel reinforcement.

The content of this paper can help the engineers to schedule and strategize suitable repair activities to avoid severe damage and possible structural failures.

## ACKNOWLEDGMENTS

The authors acknowledge the financial assistance from the New Faculty Seed Grant received from Indian Institute of Technology Madras and Fast Track grant (Sanction No. SR/FTP/ETA-0119/2011) from Department of Science and Technology (DST), Government of India. The authors acknowledge Prof. Ravindra Gettu, Prof. Manu Santhanam, Prof. Amlan K.

Sengupta, Prof. Surendra P. Shah, Ms. Payal Firodiya, staff and fellow students in the Building Technology and Construction Management Division, Department of Civil Engineering, IIT Madras for their support and timely help.

## REFERENCES

1. Life-365™ v2.2.1, Life-365 Consortium III, 2014.
2. D. Chen, S. Mahadevan, *Cem. Concr. Compos.* 30 (2008): p. 227-238.
3. D. Cusson, Z. Lounis, L. Daigle, "Improving Performance Prediction of Corroding Concrete Bridges with Field Monitoring," Proceedings of the 6th International Conference on Concrete Under Severe Conditions Environment and Loading, held June 7-9, 2010 (Merida, Mexico: CRC Press, 2010).
4. C. Suwito, Y. Xi, *Struct. Infrastruct. Eng.* 4 (2008): p. 177-192.
5. X.M. Wang, H.Y. Zhao, "The Residual Service Life Prediction of RC Structures," Proceedings of the 6th International Conference on Durability of Building Materials and Components, ed. S. Nagataki (Omiya, Japan: DBMC, 1993).
6. Z.P. Bazant, *J. Structural Division* 105 (1979): p. 1137-1153.
7. S. Morinaga, "Prediction of Service Lives of Reinforced Concrete Buildings Based on the Corrosion Rate of Reinforcing Steel," Proceedings of the Fifth International Conference on Durability of Building Materials and Components (Brighton, United Kingdom: Taylor & Francis, 1990).
8. Y. Liu, R. Weyers, *ACI Mater. J.* 95, 6 (1998): p. 675-681.
9. R.F. Stratfull, *Corrosion* 13 (1957): p. 43-48.
10. K.C. Clear, "Time to Corrosion of Reinforcing Steel in Concrete Slabs," FHA, interim report FHWA-RD-76-70, 1976.
11. C. Andrade, C. Alonso, J.A. González, "Approach to the Calculation of the Residual Service Life in Corroding Concrete Reinforcements Based on Corrosion Intensity Values," Proceedings of the 9th European Congress on Corrosion 89 (Utrecht, Netherlands: EFC, 1989).
12. "An Approach Document for Assessment of Remaining Life of Concrete Bridges," IRC SP: 60-2002 (New Delhi, India: Indian Roads Congress, 2002).
13. D.L. Spellman, R.F. Stratfull, "Chlorides and Bridge Deck Deterioration," California State Division of Highways, Materials and Research Department, Committee on Effect of Ice Control, 49th Annual Meeting, 1968.
14. K.C. Clear, *Transportation Research Record* 1211 (1992): p. 28-38.
15. K. Hladky, D.G. John, J.L. Dawson, "Development in Rate of Corrosion Measurements for Reinforced Concrete Structures," CORROSION 1989, paper no. 169 (Houston, TX: NACE International, 1989).
16. M. Ismail, M. Ohtsu, *Constr. Build. Mater.* 20 (2006): p. 458-469.
17. C.M. Hansson, B. Sorensen, "The Threshold Concentration of Chloride in Concrete for the Initiation of Reinforcement Corrosion," in *Corrosion Rates of Steel in Concrete*, eds. N.S. Berke, V. Chaker, D. Whiting, ASTM STP 1065 (Philadelphia, PA: American Society for Testing and Materials, 1990), p. 3-16.
18. N.S. Berke, D.F. Shen, K.M. Sundberg, "Comparison of the Polarization Resistance Technique to the Macrocell Corrosion Technique," in *Corrosion Rates of Steel in Concrete*, eds. N.S. Berke, V. Chaker, D. Whiting, ASTM STP 1065 (Philadelphia, PA: American Society for Testing and Materials, 1990), p. 38-51.
19. B. Pradhan, B. Bhattacharjee, *Constr. Build. Mater.* 23 (2009): p. 2346-2356.
20. P. Firodiya, A. Sengupta, R.G. Pillai, *J. Perform. Constr. Facil.* 29 (2015): ID 579.
21. J. Karuppanasamy, R.G. Pillai, "Probabilistic Estimation of Corrosion Propagation Period for Prestressed Concrete Structures Exposed to Chlorides," 4th International Conference on Durability of Concrete Structures (ICDCS 2014), held July 24-26, 2014 (West Lafayette, IN: Purdue University, 2014).
22. T.A. Soylev, M.G. Richardson, *Constr. Build. Mater.* 22 (2008): p. 609-622.

23. ASTM C204-2011, "Standard Test Methods for Fineness of Hydraulic Cement by Air-Permeability Apparatus" (West Conshohocken, PA: American Society of Testing and Materials, 2011).
24. IS:383-2002, "Specification for Coarse and Fine Aggregates from Natural Sources for Concrete" (New Delhi, India: Bureau of Indian Standards, 2002).
25. ASTM G1-2011, "Standard Practice for Preparing, Cleaning, and Evaluating Corrosion Test Specimens" (West Conshohocken, PA: American Society of Testing and Materials, 2011).
26. R.J. Detwiler, D.A. Whiting, E.S. Lagergen, *ACI Mater. J.* 96 (1999): p. 670-675.
27. EasyFit<sup>®</sup>, MathWave Technologies, 2014.